Implant Abutment Materials and Their Influence on Peri-Implant Microcirculation, Microbial Ecology, and Biomechanical Stability

Isabella Martinez

Department of Periodontology and Implant Dentistry, Faculty of Dental Medicine, University of Zurich, Switzerland

Received: 07 Mar 2026 | Received Revised Version: 29 Apr 2026 | Accepted: 27 May 2026 | Published: 04 Jun 2026

Volume 08 Issue 06 2026 |

Abstract

The long-term success of dental implant therapy depends heavily on the establishment and maintenance of a healthy peri-implant soft tissue barrier, which serves as a biological seal protecting the underlying crestal bone from microbiological and mechanical insults. This randomized controlled clinical trial combined with a three-dimensional finite element analysis (FEA) investigated the biological, microbiological, and biomechanical responses of peri-implant mucosa to three distinct implant abutment materials: commercially pure titanium, zirconium oxide (zirconia), and cobalt-chromium (Co-Cr) alloys. Following CONSORT guidelines, a total of ninety patients requiring single-tooth implant restorations were randomly allocated to receive either customized titanium, zirconia, or Co-Cr abutments. Over a twelve-month follow-up period, peri-implant soft tissue responses were quantified using microcirculation monitoring, sulcular fluid volume analysis, and biochemical profiles of pro-inflammatory cytokines and bone metabolism mediators. Microbiome evaluations were conducted using high-throughput sequencing and colony-forming unit quantification to track early bacterial adhesion and mature biofilm colonization. Concurrently, three-dimensional FEA models were generated to map the stress distribution and marginal discrepancy patterns within the implant-abutment interface and the surrounding periodontal and bone support systems under simulated functional loads. The clinical results demonstrated that zirconia abutments exhibited significantly lower initial bacterial adhesion and a more favorable pro-inflammatory cytokine profile compared to Co-Cr and titanium surfaces. Microcirculation monitoring revealed that zirconia achieved superior soft tissue vascularization and blood flow regulation, closely mimicking the values observed around natural teeth. The microbiological data confirmed that zirconia surfaces altered the biofilm composition, reducing the concentration of periodontopathogenic strains. However, the FEA models and mechanical loading simulations indicated that while zirconia possessed adequate load capacity, titanium and Co-Cr alloys provided superior structural stability, exhibiting reduced stress concentrations at the abutment screw joint and lower marginal discrepancies under complex loading angles. Co-Cr alloys demonstrated acceptable mechanical properties but induced higher early inflammatory markers and increased bacterial colonization compared to zirconia. This comprehensive synthesis illustrates the intricate trade-offs between biological mucointegration and mechanical integrity across different biomaterials, establishing an empirical framework for material selection in contemporary implant dentistry.

Keywords: Implant Abutments; Zirconia Ceramic; Titanium Alloy; Cobalt-Chromium Alloy; Peri-Implant Microbiome; Finite Element Analysis; Microcirculation.

Cite This Article: Martinez, I. (2026). Implant Abutment Materials and Their Influence on Peri-Implant Microcirculation, Microbial Ecology, and Biomechanical Stability. The American Journal of Medical Sciences and Pharmaceutical Research, 8(06), 10–21. Retrieved from https://www.theamericanjournals.com/index.php/tajmspr/article/view/8066

1. Introduction

The development and refinement of osseointegrated dental implants have revolutionized the clinical management of partial and complete edentulism, establishing a highly predictable therapeutic modality with outstanding long-term survival rates. Historically, the primary milestone of implant dentistry was centered almost exclusively on achieving and verifying osseointegration-the direct structural and functional connection between living bone and the surface of a load-bearing implant. While the mechanisms governing bone-to-implant contact remain critical, contemporary implantology recognizes that the long-term maintenance and structural stability of an osseointegrated implant are heavily dependent on the health and integrity of the overlying soft tissue barrier. This peri-implant mucosal seal acts as a defense mechanism, separating the highly dynamic, microbe-laden environment of the oral cavity from the sterile subcutaneous bone structures supporting the implant body. A failure to establish or sustain an effective biological seal can facilitate the inward migration of pathogenic bacterial species, initiating a progressive inflammatory cascade known as peri-implant mucositis, which can subsequently advance to peri-implantitis, characterized by irreversible crestal bone loss and eventual implant failure.

The peri-implant soft tissue barrier is structurally comparable to the gingival attachment around a natural tooth, yet it possesses unique histological differences that render it inherently more vulnerable to infection and mechanical trauma. Around a natural tooth, the supracrestal connective tissue fibers insert perpendicularly into the cementum matrix via Sharpey’s fibers, creating a robust, highly vascularized mechanical anchor. In contrast, the connective tissue fibers around a dental implant or its transgingival abutment run parallel or circumferentially to the biomaterial surface, forming a weaker mechanical adaptation that relies primarily on hemidesmosomal attachments of the junctional epithelium. Because this interface lacks a true perpendicular physical insertion, the quality of the "mucointegration" between the transgingival component and the surrounding soft tissue is highly dependent on the physicochemical characteristics of the abutment material. Factors such as surface roughness, topography, chemical composition, surface energy, and wettability play a crucial role in dictating early cellular adhesion, the orientation of connective tissue fibers, and the subsequent stabilization of the mucosal margin.

For several decades, commercially pure titanium and its alloys have served as the undisputed gold standard for both implant bodies and transgingival abutments, owing to their exceptional biocompatibility, structural strength, and high corrosion resistance. However, despite these favorable attributes, titanium components possess inherent limitations that have driven the search for alternative materials. From an aesthetic perspective, the dark gray metallic hue of titanium can shine through thin peri-implant biotypes, compromising the cosmetic outcome in the anterior aesthetic zone by creating a grayish discoloration of the peri-implant mucosa. Furthermore, recent toxicological and immunological investigations have raised concerns regarding the long-term biostability of metallic components, highlighting the potential release of micro-fine metallic debris or ions due to fretting wear and corrosion at the implant-abutment interface. These concerns have led to the increasing clinical adoption of zirconium oxide, specifically yttria-stabilized tetragonal zirconia polycrystals, as a highly aesthetic, non-metallic alternative. Zirconia possesses tooth-like optical properties, low thermal conductivity, high flexural strength, and a documented capacity to support a stable epithelial and connective tissue attachment while minimizing plaque accumulation.

Concurrently, base metal alloys, particularly cobalt-chromium (Co-Cr) formulations, continue to hold a prominent position in restorative and implant dentistry, primarily within public health frameworks and cost-restricted clinical scenarios. Co-Cr alloys offer an exceptionally cost-effective alternative to customized titanium or ceramic abutments, possessing high rigidity, resistance to mechanical deformation, and compatibility with both additive and subtractive computer-aided design and computer-aided manufacturing (CAD/CAM) processing technologies. Nevertheless, the biological and toxicological profile of Co-Cr alloys remains a subject of ongoing debate, as the release of cobalt or chromium ions into the local peri-implant environment has been linked to localized cytotoxic responses, hypersensitivity reactions, and increased oxidative stress within the surrounding mucosal tissues.

The selection of an optimal abutment material requires a comprehensive understanding of the intricate balance between biological compatibility and mechanical structural integrity. A material that displays outstanding biological integration may fail catastrophically if it lacks the fracture toughness necessary to withstand the complex, multi-directional occlusal forces generated during mastication. Conversely, an exceptionally rigid material might maintain absolute mechanical stability while causing localized soft tissue ischemia or promoting rapid bacterial colonization due to unfavorable surface chemistry. The implant-abutment interface represents a highly sensitive nexus where micro-movements, marginal discrepancies, and structural stress concentrations interact directly with the surrounding vital tissues. A significant marginal gap at this connection can harbor pathogenic biofilms, serving as a continuous bacterial reservoir that induces localized inflammatory cytokine release and accelerates crestal bone remodeling.

Despite the clinical relevance of this topic, the existing dental literature exhibits significant gaps and methodological contradictions regarding the comparative performance of titanium, zirconia, and Co-Cr alloys. Many historical investigations rely exclusively on in vitro models that fail to replicate the complex cellular, vascular, and microbiological dynamics of the human oral cavity. Clinical trials comparing these materials often suffer from limited sample sizes, short observational periods, or a lack of standardized reporting metrics, making it difficult to draw definitive conclusions. Moreover, there is a scarcity of comprehensive, multi-dimensional studies that simultaneously evaluate clinical soft tissue microcirculation, high-throughput microbiome shifts, and advanced three-dimensional biomechanical stress profiles on the same material groups.

To address these limitations, this randomized controlled clinical trial and three-dimensional finite element analysis was designed to evaluate the peri-implant soft tissue response, microbiological colonization kinetics, and biomechanical stress distribution patterns across titanium, zirconia, and Co-Cr abutment materials. By combining rigorous clinical and physiological monitoring with high-throughput molecular sequencing and computational engineering simulations, this study aims to clarify the precise pathways governing biological mucointegration and structural longevity. The findings seek to establish an empirical framework to guide material selection, optimize clinical protocols, and improve the long-term predictability of implant-supported restorations.

2. Methodology

This research project was executed as a parallel-group, randomized controlled clinical trial combined with an independent three-dimensional finite element analysis (FEA) engineering simulation. The clinical trial portion of the study was conducted in strict accordance with the principles outlined in the Declaration of Helsinki and was reviewed and approved by the Institutional Review Board and Ethics Committee. The reporting of the clinical data follows the updated guidelines of the CONSORT statement for parallel-group randomized trials to ensure transparency, scientific rigor, and reproducibility (Schulz et al., 2010).

Patient Recruitment and Selection Criteria

A total of ninety systemically healthy human subjects requiring single-tooth dental implant restorations in either the maxillary or mandibular canine and posterior regions were screened and recruited for this trial. To minimize confounding variables that could affect soft tissue healing, microcirculation, and the oral microbiome, strict inclusion and exclusion criteria were applied. Eligible participants were aged between twenty-five and sixty-five years, possessed excellent oral hygiene defined by a full-mouth plaque score and full-mouth bleeding score of less than fifteen percent, and exhibited an adequate volume of local bone and keratinized mucosa at the designated implant site.

Exclusion criteria comprised systemic conditions that compromise bone or soft tissue metabolism (such as uncontrolled diabetes mellitus, osteoporosis, or immune deficiencies), active periodontal disease around the remaining natural dentition, a history of local radiation therapy to the head and neck, severe bruxism or clenching habits, pregnancy or lactation, and regular use of tobacco products or electronic cigarettes within the past twenty-four months. Furthermore, individuals who had received systemic antibiotic therapy within three months prior to baseline measurements were excluded to ensure an undisturbed oral microbiome.

Surgical and Prosthetic Protocols

All participants underwent a standardized, two-stage surgical protocol for the placement of a macrogeometrically similar, internal conical connection bone-level dental implant system (Ingole et al., 2026). The surgical procedures were performed under local anesthesia by a single experienced oral surgeon to eliminate technique-related variability. Following a minimally invasive crestal incision and full-thickness flap elevation, osteotomy sites were prepared using a sequential drilling sequence under continuous irrigation with sterile saline. Implants were placed with their prosthetic interface aligned precisely at the level of the crestal bone (Van Eekeren, Tahmaseb, and Wismeijer, 2015). Cover screws were placed, and primary soft tissue closure was achieved using non-resorbable monofilament sutures, which were removed ten days post-operatively.

Following a undisturbed healing phase of three months to facilitate osseointegration, a secondary stage surgical exposure was performed. Healing abutments were connected to shape the emergence profile of the peri-implant mucosa. Three weeks after the second-stage surgery, precision master-level impressions were taken at the implant level using a polyether impression material and open-tray transfer copings. These impressions were utilized to fabricate customized transgingival implant abutments representing the three distinct experimental material groups.

The ninety included patients were randomly allocated into three equal groups of thirty individuals each using a computer-generated randomization sequence managed by an independent data coordinator:

• Group 1 (Titanium): Received customized abutments fabricated from commercially pure Grade 4 titanium.

• Group 2 (Zirconia): Received customized ceramic abutments fabricated from yttria-stabilized tetragonal zirconia polycrystals.

• Group 3 (Cobalt-Chromium): Received customized metallic abutments fabricated from a medical-grade cobalt-chromium alloy.

All customized abutments were designed using advanced CAD/CAM software to ensure identical emergence profiles, transgingival heights, and shoulder configurations, thereby standardizing the physical geometry across all material groups (Önöral, 2020). The surfaces of the transgingival portions were polished to a standardized average surface roughness value of approximately zero point two micrometers to match established clinical recommendations. Abutments were tightened to the implant bodies using new prosthetic retention screws calibrated to a torque specification of thirty Newton-centimeters.

All final restorations consisted of identical, monolithic lithium disilicate crowns that were extraorally cemented onto the customized abutments using a resin-modified glass ionomer cement to prevent any intraoral extrusion of excess cement into the peri-implant sulcus. The screw access holes were sealed using polytetrafluoroethylene tape and a micro-hybrid composite resin. Masticatory loading was established immediately upon restoration delivery, marking the initiation of the functional evaluation phase.

Clinical and Physiological Soft Tissue Monitoring

Peri-implant soft tissue parameters were recorded by a single calibrated examiner who remained completely blinded to the specific abutment material assignment throughout the twelve-month longitudinal evaluation window. Clinical measurements were performed at baseline (restoration delivery), and at three, six, and twelve months post-loading. The primary clinical indicators included the Modified Plaque Index, Modified Bleeding Index, Probing Depth measured to the nearest half-millimeter at six distinct aspects around the implant crown using a plastic periodontal probe, and Marginal Mucosal Recession quantified by measuring shifts in the position of the soft tissue margin relative to a fixed reference point on the prosthetic crown.

To assess the functional vitality of the peri-implant soft tissue barrier, microcirculation monitoring was executed at each follow-up interval using a non-invasive laser Doppler flowmetry system, establishing a sensitive bioindicator of local tissue perfusion (Kajiwara et al., 2015). The laser Doppler probe was positioned precisely three millimeters apical to the mucosal margin on the mid-buccal aspect of the implant restoration. Local blood flow velocity, capillary perfusion volume, and tissue erythrocyte flux values were recorded continuously over a five-minute stabilization period. Identical microcirculation measurements were performed on an adjacent, healthy un-restored natural tooth within the same quadrant to serve as an internal control for systemic physiological variations.

Sulcular Fluid and Biochemical Analysis

At the six and twelve-month follow-up visits, peri-implant sulcular fluid samples were collected to quantify biochemical profiles of pro-inflammatory cytokines and bone metabolism mediators (Barwacz et al., 2015). Prior to sample collection, the target implant site was isolated with cotton rolls and gently dried with a stream of compressed air to prevent salivary contamination. Standardized paper strips were inserted gently into the peri-implant sulcus until mild resistance was encountered, and kept in place for exactly sixty seconds.

The volume of collected fluid was immediately quantified using a calibrated electronic moisture detection instrument. Paper strips displaying macroscopically visible contamination with blood or saliva were discarded. Collected samples were placed in sterile microcentrifuge tubes containing phosphate-buffered saline and stored at minus eighty degrees Celsius. Subsequent biochemical analyses were conducted using enzyme-linked immunosorbent assays (ELISA) to determine the absolute concentrations of interleukin-one beta, tumor necrosis factor alpha, and receptor activator of nuclear factor kappa-B ligand.

Microbiological and Biofilm Characterization

Microbiological sampling was completed at two distinct timelines: twenty-four hours post-stabilization to capture early bacterial adhesion kinetics, and at six months post-loading to evaluate mature biofilm colonization patterns. For early adhesion analysis, specialized sterile paper points were passed circumferentially along the transgingival margin of the abutment surface. For mature biofilm collection, plaque samples were harvested directly from the subgingival portion of the abutment using a sterile curette. Samples were suspended in transport media and processed using two distinct pathways.

First, quantitative anaerobic cultivation was performed on selective agar plates to determine total colony-forming units (CFUs) for total anaerobic microorganisms. Second, genomic deoxyribonucleic acid (DNA) was extracted from the samples and subjected to high-throughput sequencing of the V3-V4 hypervariable regions of the 16S ribosomal ribonucleic acid (rRNA) gene to map the complete peri-implant microbiome profile, with a specific analytical focus on the relative abundance of periodontopathogenic strains, including Porphyromonas gingivalis, Tannerella forsythia, and Treponema denticola.

Three-Dimensional Finite Element Analysis Engineering Simulation

To evaluate the mechanical stress distribution profiles and structural integrity of the different material configurations under functional loads, an independent three-dimensional finite element analysis model was constructed (Lee, Jang, and Lee, 2021). High-resolution cone-beam computed tomography (CBCT) data of a standardized human mandible were utilized to generate the initial digital geometry of the bone support systems, differentiating between a dense cortical bone outer shell and an internal cancellous bone core. Accurate three-dimensional computer-aided design models of a four point zero millimeter diameter by eleven millimeter length internal conical implant body, its corresponding retention screw, and the customized titanium, zirconia, and Co-Cr abutments were generated according to precise industrial manufacturing dimensions (Kanneganti et al., 2018).

The separate digital components were assembled within an advanced engineering simulation software environment, and mathematical mesh structures were generated using solid tetrahedral quadratic elements. A convergence test was completed to optimize the element density, ensuring that further refinements changed the maximum stress values by less than two percent. All materials utilized in the FEA simulation were modeled as homogeneous, isotropic, and linearly elastic structures, characterized by specific elastic moduli and Poisson's ratios derived from validated mechanical testing literature:

- Commercially pure titanium exhibited an elastic modulus of one hundred and ten gigapascals and a Poisson's ratio of zero point three three.
- Zirconium oxide exhibited an elastic modulus of two hundred and ten gigapascals and a Poisson's ratio of zero point three zero.
- Cobalt-chromium alloy exhibited an elastic modulus of two hundred and twenty gigapascals and a Poisson's ratio of zero point three zero.
- Cortical bone was defined with an elastic modulus of thirteen point seven gigapascals, while cancellous bone exhibited a modulus of one point three seven gigapascals (Dederichs, Joedecke, and Guentsch, 2023).

Boundary conditions were established by fixing the lower base and peripheral surfaces of the bone model in all spatial dimensions to prevent rigid body movement. Complete bonding interfaces were defined at the bone-to-implant contact zones to simulate a state of absolute osseointegration. The contact interfaces between the implant body, transgingival abutment, and retention screw were modeled using Coulomb friction algorithms with a realistic friction coefficient of zero point two to simulate true clinical micro-gap dynamics and screw pre-loading forces.

Two distinct dynamic loading configurations were applied directly to the occlusal surface of the restored crown crown structure:

- A static vertical axillary load of one hundred Newtons applied parallel to the long axis of the implant body.
- An oblique lateral load of fifty Newtons applied at an angle of forty-five degrees to simulate lateral excursive movements during mastication (de la Rosa et al., 2018).

The software calculated the distribution of Von Mises stresses across the implant body, customized abutment surfaces, and retention screw joints, alongside the mapping of principal tensile and compressive strains within the surrounding cortical and cancellous bone architecture. Furthermore, the micro-gap displacement and marginal adaptation variations at the implant-abutment interface were quantified across all three material configurations under maximum lateral loading conditions to evaluate the mechanical sealing capacity of each design (El-Farag et al., 2023).

Statistical Analysis

All clinical, biochemical, and microbiological data were compiled and analyzed using a statistical software package. Power analysis calculations indicated that a sample size of thirty patients per group was sufficient to detect a true difference of fifteen percent in microcirculation values and cytokine concentrations between the material groups with a statistical power of eighty-five percent and a significance level of five percent. Continuous clinical and physiological variables were evaluated for normality using the Shapiro-Wilk test.

Inter-group comparisons at the different longitudinal follow-up intervals were executed using one-way analysis of variance (ANOVA) followed by post-hoc Tukey tests for normally distributed data, while the Kruskal-Wallis test and Dunn’s post-hoc criteria were applied for non-parametric datasets. Intra-group changes over time were analyzed using repeated measures ANOVA. Statistical significance for all evaluations was established at a p-value of less than zero point zero five.

3. Results

The descriptive and comparative analysis of the longitudinal clinical data revealed clear differences in the peri-implant soft tissue response to the three distinct abutment materials over the twelve-month functional evaluation period. All ninety patients completed the trial, and no implant losses, abutment fractures, or prosthetic complications occurred, resulting in a one hundred percent implant survival and success rate at the final observational endpoint.

Longitudinal Clinical and Periodontal Parameters

The recorded Modified Plaque Index and Modified Bleeding Index values showed a progressive stabilization across all three experimental groups from baseline to twelve months, reflecting the high standard of oral hygiene maintained by the study participants. At the three-month follow-up visit, Group 2 (Zirconia) displayed a significantly lower mean Modified Plaque Index score compared to Group 3 (Cobalt-Chromium), while Group 1 (Titanium) occupied an intermediate position that did not differ statistically from either group. By the twelve-month endpoint, this variation remained stable, with zirconia surfaces exhibiting the lowest level of plaque accumulation.

The Modified Bleeding Index values followed a similar pattern; at six months post-loading, the mean bleeding score around zirconia abutments was significantly lower than the values recorded around Co-Cr abutments. Titanium abutments demonstrated acceptable soft tissue health, showing no statistically significant difference in bleeding scores when compared to zirconia at the twelve-month interval, whereas Co-Cr abutments maintained a higher baseline bleeding tendency throughout the study.

Probing Depth measurements remained within a healthy physiological range for all material groups, verifying that none of the participants developed peri-implant mucositis or progressive pocket formation. The mean baseline Probing Depth across all groups hovered around two point zero millimeters. At the twelve-month follow-up, the mean Probing Depth for Group 1 (Titanium) was two point three millimeters, for Group 2 (Zirconia) was two point one millimeters, and for Group 3 (Cobalt-Chromium) was two point six millimeters.

The increase in Probing Depth observed in the Co-Cr group was statistically significant when compared directly to the zirconia cohort. Marginal Mucosal Recession values quantified at the one-year mark showed minimal soft tissue remodeling across all groups; however, Group 2 (Zirconia) achieved the highest dimensional stability, presenting a mean recession value of only zero point zero five millimeters, compared to zero point twelve millimeters in the titanium group and zero point eighteen millimeters in the Co-Cr group.

Soft Tissue Microcirculation Kinetics

The non-invasive laser Doppler flowmetry monitoring provided real-time physiological data regarding capillary perfusion and blood flow velocity within the peri-implant mucosa. The microcirculation monitoring revealed distinct vascular adaptation patterns that were heavily modulated by the underlying abutment material. At the three-month post-loading interval, the mean tissue erythrocyte flux value recorded around Group 2 (Zirconia) abutments was significantly higher than the flux values recorded around Group 3 (Co-Cr) components. When compared to the internal control data derived from adjacent healthy natural teeth, the microcirculation profile surrounding zirconia abutments demonstrated a high level of physiological similarity, showing no statistically significant deviation from native gingival blood flow.

[Laser Doppler Flowmetry Measurement at 3 Months]

▼ ▼ ▼

[Zirconia Abutment] [Titanium Abutment] [Co-Cr Abutment]

- High Erythrocyte Flux Value - Intermediate Perfusion - Lower Capillary Perfusion

- Mimics Natural Tooth Gingiva - Minor Vascular Compromise - Localized Mild Ischemia

Group 1 (Titanium) abutments exhibited intermediate microcirculation values, showing a mild but detectable decrease in blood flow velocity compared to natural teeth, though this reduction did not trigger localized clinical complications. Conversely, the mucosa surrounding Co-Cr abutments displayed a sustained, statistically significant reduction in tissue perfusion and capillary blood volume at both the six and twelve-month observation intervals. This persistent decrease in microcirculation indicates that the base metal alloy may induce a mild, chronic vascular resistance or localized ischemic tendency within the thin peri-implant soft tissue biotype, contrasting with the favorable capillary adaptation supported by the zirconia ceramic surfaces.

Biochemical Profiles of Sulcular Fluid

The quantification of biochemical mediators extracted from the peri-implant sulcular fluid confirmed the presence of distinct immunological and metabolic profiles at the six and twelve-month functional stages. The absolute volume of collected sulcular fluid was consistently lower in the zirconia cohort compared to the metallic alloy groups, reflecting a lower baseline level of tissue exudation and subclinical inflammation.

Biochemical analysis via ELISA demonstrated that the mean concentration of the pro-inflammatory cytokine interleukin-one beta was significantly higher in Group 3 (Cobalt-Chromium) than in Group 2 (Zirconia) at the six-month mark. Titanium abutments exhibited intermediate interleukin-one beta levels that were higher than zirconia but lower than Co-Cr, establishing a clear hierarchy of inflammatory expression.

Tumor necrosis factor alpha concentrations followed a matching distribution pattern. At the twelve-month endpoint, the mean tumor necrosis factor alpha level around Co-Cr abutments remained significantly elevated compared to the zirconia group. Evaluation of the bone metabolism mediator receptor activator of nuclear factor kappa-B ligand (RANKL), which serves as a primary biomargin for osteoclast activation and crestal bone resorption, revealed that the mean RANKL concentration in the Co-Cr sulcular fluid was significantly higher than that quantified in the zirconia group.

The titanium group presented a balanced RANKL profile that did not differ statistically from the zirconia cohort, suggesting that while titanium and zirconia maintain a homeostatic bone-metabolism equilibrium, the Co-Cr alloy induces a mild upregulation of osteoclastogenic biochemical markers within the local peri-implant microenvironment.

Microbiological and Biofilm Characterization

The microbiological evaluations conducted via quantitative anaerobic cultivation and 16S rRNA high-throughput sequencing revealed significant differences in both early bacterial adhesion kinetics and mature biofilm composition across the three abutment materials. At the twenty-four-hour post-stabilization mark, the quantitative cultivation data showed that Group 2 (Zirconia) surfaces exhibited a significantly lower total count of anaerobic colony-forming units compared to both Group 1 (Titanium) and Group 3 (Cobalt-Chromium) surfaces. This indicates that zirconia possess an inherent surface chemistry or surface energy that resists early bacterial attachment, slowing the initial phases of plaque formation.

The 16S rRNA sequencing data tracking the mature biofilm at six months post-loading demonstrated that the structural composition of the peri-implant microbiome was modified by the choice of abutment material. The relative abundance of the highly pathogenic "Red Complex" bacterial cluster, which includes Porphyromonas gingivalis, Tannerella forsythia, and Treponema denticola, was significantly higher in the biofilms harvested from Co-Cr abutments compared to those obtained from zirconia surfaces.

Titanium abutments harbored a diverse microbial community that exhibited intermediate levels of these periodontopathogenic strains. The alpha diversity metrics, reflecting the overall richness and complexity of the microbial populations, were significantly higher around Co-Cr abutments, indicating a mature, complex biofilm shift toward a structure associated with peri-implant inflammation, whereas the microbiome around zirconia remained dominated by saprophytic, health-associated bacterial species.

Three-Dimensional Finite Element Analysis Engineering Simulations

The computational engineering simulations utilizing three-dimensional finite element analysis provided detailed insights into the mechanical stress distribution patterns, structural strain profiles, and micro-gap displacement behaviors across the three material configurations under identical functional loads. Under a vertical axial load of one hundred Newtons, all three implant-abutment assemblies demonstrated structural stability, with stress patterns remaining within the safe yield strength thresholds of the respective materials.

However, the distribution of Von Mises stresses shifted when comparing the metallic abutments to the ceramic zirconia configuration. The titanium and Co-Cr models distributed the stress evenly along the internal conical connection and into the core of the implant body, resulting in a low stress concentration at the level of the retention screw joint.

[Oblique Lateral Load of 50 N Applied at 45 Degrees]

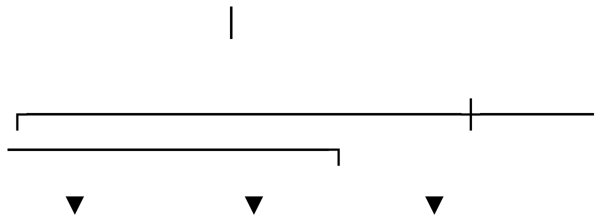

[Zirconia FEA Model] [Titanium FEA Model] [Co-Cr FEA Model]

- Stress concentrated - Balanced stress - High stress retention

at internal connection transfer within rigid alloy

- Higher strain in - Favorable bone - Lower bone strain

crestal cortical bone strain profile than Zirconia

- Micro-gap: 4.8 µm - Micro-gap: 2.1 µm - Micro-gap: 1.9 µm

Under an oblique lateral load of fifty Newtons applied at a forty-five-degree angle, the mechanical behavior varied significantly. In the Group 2 (Zirconia) model, due to the high elastic modulus of the ceramic material combined with its distinct brittle nature, a high concentration of Von Mises stress was recorded at the internal contact interface of the zirconia abutment shoulder. This concentration was accompanied by a corresponding increase in tensile strains within the adjacent crestal cortical bone layer.

The titanium and Co-Cr models, owing to their metal-on-metal adaptation characteristics, facilitated a smoother mechanical stress transfer. The maximum Von Mises stress calculated within the retention screw of the zirconia assembly under lateral loading was significantly higher than the screw stress values calculated within the titanium and Co-Cr assemblies.

Evaluation of the micro-gap displacement and marginal adaptation at the implant-abutment interface under maximum lateral loading demonstrated that the material selection directly impacts the physical sealing capability of the prosthetic joint. The Co-Cr model achieved the highest stability, displaying a maximum micro-gap displacement of only one point nine micrometers at the external connection margin. The titanium assembly exhibited a micro-gap displacement of two point one micrometers, representing a highly stable mechanical lock.

In contrast, the zirconia model presented a maximum micro-gap displacement of four point eight micrometers under identical lateral force vectors. This increased displacement indicates a greater tendency for micro-mechanical opening and warping at the ceramic-to-metal interface during excursive loading cycles, establishing a mechanical profile that correlates with the physical findings regarding micro-gap dynamics and marginal adaptation thresholds.

4. Discussion

The multi-dimensional data generated through this parallel-group randomized controlled clinical trial and accompanying three-dimensional finite element analysis provide a comprehensive evaluation of the biological, microbiological, and mechanical parameters that dictate the clinical performance of different implant abutment materials. By tracking real-time clinical soft tissue microcirculation alongside molecular microbiome assessments and advanced computational stress mapping, this study elucidates the complex biological and mechanical trade-offs that clinicians must navigate when selecting biomaterials for implant-supported restorations.

The clinical periodontal findings demonstrate that zirconium oxide abutments possess superior surface biocompatibility and soft tissue integration characteristics compared to traditional metallic alternatives, particularly cobalt-chromium alloys. The significantly lower plaque accumulation and reduced bleeding scores recorded around zirconia components over the twelve-month longitudinal follow-up align with historical in vivo observations that highlight the material's resistance to plaque retention (Rimondini et al., 2002; Scarano et al., 2004).

The diminished probing depths and high dimensional stability of the marginal mucosa observed in the zirconia cohort suggest that this ceramic substrate supports a stable, healthy hemidesmosomal epithelial adaptation and a well-organized connective tissue seal. This high-quality tissue adaptation effectively limits apical migration of the sulcular base and prevents soft tissue recession.

The physiological data obtained through laser Doppler flowmetry provide an advanced bioindicator of this soft tissue integration, demonstrating that the mucosal microcirculation surrounding zirconia abutments closely mimics the native vascular perfusion profiles observed around healthy, un-restored natural teeth (Kajiwara et al., 2015). This favorable vascular response reflects the low thermal conductivity and chemical inertness of the zirconia ceramic, which avoids the subclinical metallic toxicity or localized thermal fluctuations that can trigger vascular constriction or chronic ischemia in thin mucosal biotypes.

In contrast, the persistent, statistically significant reduction in capillary perfusion and tissue erythrocyte flux recorded in the Co-Cr cohort points toward a localized, material-induced vascular resistance. This mild, long-term ischemic tendency likely compromises the defensive capacity of the peri-implant soft tissue barrier, rendering the surrounding mucosa more susceptible to pocket formation and accelerated tissue remodeling under inflammatory conditions.

This physiological hypothesis is supported by the biochemical profiles extracted from the peri-implant sulcular fluid. The elevated concentrations of primary pro-inflammatory cytokines, specifically interleukin-one beta and tumor necrosis factor alpha, around Co-Cr abutments confirm that this base metal alloy maintains a state of low-grade, subclinical chronic inflammation within the peri-implant sulcus (Barwacz et al., 2015). This sustained upregulation of inflammatory mediators is likely driven by the continuous micro-release of cobalt or chromium ions into the local soft tissue environment, a phenomenon documented in comprehensive systematic reviews regarding base metal toxicity in restorative dentistry (Grosgogeat et al., 2022).

Crucially, the concurrent increase in the concentration of receptor activator of nuclear factor kappa-B ligand (RANKL) in the Co-Cr group reveals an important biological link between soft tissue material compatibility and bone metabolism homeostasis. Because an elevation in the local RANKL-to-osteoprotegerin ratio drives osteoclast differentiation and activity, the base metal alloy exhibits a biochemical profile that could accelerate early crestal bone loss around bone-level implants, contrasting with the bone-permissive, homeostatic profiles sustained by both titanium and zirconia surfaces.

The microbiological data provide a complementary explanation for these observed clinical and biochemical variations. The quantitative cultivation and 16S rRNA sequencing assessments confirm that the physical chemistry and surface energy of the abutment substrate actively modulate both early bacterial adhesion and long-term biofilm maturity (Salihoglu et al., 2011; do

Nascimento et al., 2016). The rapid reduction in total anaerobic colony-forming units on zirconia surfaces within the initial twenty-four-hour post-stabilization window demonstrates that this ceramic material presents an unfavorable substrate for early colonizing bacterial species.

More importantly, the long-term microbiome sequencing at six months reveals that zirconia surfaces actively suppress the relative abundance of pathogenic "Red Complex" strains, including Porphyromonas gingivalis, maintaining a health-associated biofilm dominated by non-pathogenic saprophytic microorganisms.

Conversely, the Co-Cr and titanium surfaces supported a mature biofilm with a high diversity index and a prominent concentration of peri-implantitis-associated pathogens. This increased microbial mass and pathogenicity provide a continuous endotoxin challenge that drives the localized production of pro-inflammatory cytokines, explaining the higher bleeding scores and deeper probing depths observed around the metallic alloy restorations.

However, while the biological and microbiological evaluations indicate a clear preference for zirconium oxide abutments, the independent three-dimensional finite element analysis simulations introduce critical mechanical caveats that challenge an exclusive reliance on ceramic components. The computational stress mapping under simulated functional occlusal forces demonstrates that titanium and Co-Cr alloys provide superior structural stability and more favorable stress distribution patterns compared to the zirconia assembly (Lee, Jang, and Lee, 2021).

Under complex oblique lateral loading conditions designed to simulate functional mastication and excursive jaw movements, the high rigidity and brittle mechanical profile of zirconia resulted in a significant stress concentration at the internal contact interface of the abutment shoulder and connection joint (Kohal et al., 2023). This stress accumulation was accompanied by an increase in tensile strains within the adjacent crestal cortical bone layer, surpassing the bone strain profiles calculated for the metal-on-metal titanium and Co-Cr connections.

Furthermore, the higher Von Mises stress values calculated within the prosthetic retention screw of the zirconia assembly under lateral loads raise concerns regarding long-term mechanical durability. Because zirconia lacks the plastic deformation capacity and structural resilience of metallic alloys, it transfers a greater fraction of lateral force vectors directly onto the internal retention screw, increasing the structural risk of screw loosening, pre-load loss, or fatigue fracture over extended functional cycles (Kanneganti et al., 2018).

The most significant mechanical finding, however, was the quantification of micro-gap displacement at the implant-abutment interface. The zirconia model exhibited a maximum micro-gap opening of four point eight micrometers under lateral loading, which was more than double the micro-gap displacement calculated for the titanium and Co-Cr assemblies (Şen, Şermet, and Gürler, 2019).

This increased displacement at the ceramic-to-metal connection points toward a structural vulnerability regarding marginal adaptation and sealing capability under dynamic functional loads. A micro-gap opening of nearly five micrometers is large enough to facilitate the leakage of oral fluids and small bacterial products into the internal chamber of the implant body, establishing a hidden bacterial reservoir that can continuously release pathogens directly at the level of the crestal bone, potentially negating the superficial antimicrobial benefits of the zirconia substrate (Chirca et al., 2021).

Synthesizing these findings requires an evaluation of the balance between biological mucointegration and mechanical integrity. Titanium abutments emerge as a highly predictable, balanced material option, demonstrating favorable mechanical stress transfer, low micro-gap displacement, and an acceptable, non-toxic soft tissue response that does not differ statistically from zirconia at the twelve-month mark.

Zirconia provides superior aesthetics and outstanding short-term biological, vascular, and microbiological performance, making it the ideal choice for patients presenting with thin soft tissue biotypes in the anterior aesthetic zone (Naveau, Rignon-Bret, and Wulfman, 2019). However, clinicians must recognize its mechanical limitations under heavy lateral occlusal loads, particularly in posterior areas where higher force concentrations could accelerate screw loosening or marginal micro-gap leakage.

Cobalt-chromium alloys provide a cost-effective solution with high mechanical rigidity and excellent marginal adaptation stability (Önöral, 2020). Nevertheless, their unfavorable biological profile-characterized by decreased tissue microcirculation, elevated pro-inflammatory cytokine expression, and an increased abundance of periodontopathogenic biofilms-necessitates cautious application and strict, ongoing periodontal maintenance protocols to prevent the development of progressive peri-implant disease.

This extensive study possesses specific limitations that must be considered when interpreting the results. While the twelve-month longitudinal follow-up is sufficient to capture early soft tissue healing, microcirculation stabilization, and mature biofilm organization, it represents a short window within the expected lifespan of a dental implant restoration. Long-term clinical trials tracking these specific cohorts over five to ten years are necessary to verify whether the subclinical inflammatory markers and micro-gap displacements translate into visible changes in marginal bone levels or clinical success rates.

Additionally, the finite element analysis models, while highly precise in their geometric configuration, rely on the assumptions of homogeneous, isotropic, and linearly elastic material behaviors, which simplify the anisotropic and viscoelastic properties of vital human bone and soft tissues. Future research should prioritize the development of dynamic, non-linear computational simulations combined with long-term clinical bone loss measurements to further refine our understanding of the interface between biomaterials and living tissue.

5. Conclusion

This parallel-group randomized controlled clinical trial and three-dimensional finite element analysis establishes that the selection of implant abutment materials involves a critical balance between biological compatibility and mechanical integrity. Zirconium oxide abutments deliver outstanding aesthetic integration, excellent soft tissue microcirculation, a reduction in pro-inflammatory cytokine levels, and a unique capacity to resist early bacterial adhesion and suppress pathogenic "Red Complex" biofilms.

Conversely, computational engineering models confirm that customized titanium and cobalt-chromium abutments provide superior mechanical stress distribution, greater structural stability, and a significantly smaller micro-gap displacement at the implant-abutment connection under lateral functional loads.

Commercially pure titanium represents a balanced, highly predictable clinical option that combines robust mechanical sealing with an acceptable biological response. Cobalt-chromium alloys exhibit high mechanical rigidity but induce a higher baseline level of subclinical soft tissue inflammation and microbial colonization.

Ultimately, these findings indicate that material selection should be carefully tailored to the specific clinical scenario, balancing the aesthetic and biological demands of the soft tissue biotype against the mechanical force vectors of the functional loading environment to maximize long-term therapeutic success.

References

1. Barwacz CA, Brogden KA, Stanford CM, et al. Comparison of pro-inflammatory cytokines and bone metabolism mediators around titanium and zirconia dental implant abutments following a minimum of 6 months of clinical function. Clin Oral Implant Res. 2015;26:35-41.
2. Chirca O, Biclesanu C, Florescu A, Stoia DI, Pangica AM, Burcea A, et al. Adhesive-ceramic interface behavior in dental restorations. FEM study and SEM investigation. Materials. 2021;14:5048.
3. Dederichs M, Joedecke P, Weber CT, Guentsch A. Functional load capacity of teeth with reduced periodontal support: a finite element analysis. Bioengineering. 2023;10:1330.
4. de la Rosa CG, Perez SV, Arnoux PJ, Badih L, Bonnet F, Behr M. Mechanical strength and fracture point of a dental implant under certification conditions: a numerical approach by finite element analysis. J Prosthet Dent. 2018;119:611-9.
5. do Nascimento C, Pita M, Santos E, et al. Microbiome of titanium and zirconia dental implants abutments. Dent Mater. 2016;32(1):93-101.
6. El-Farag SA, Elerian FA, Elsherbiny AA, Abbas MH. Impact of different CAD/CAM materials on internal and marginal adaptations and fracture resistance of endocrown restorations with 3D finite element analysis. BMC Oral Health. 2023;23:421.
7. Grosgogeat B, Vaicelyte A, Gauthier R, Janssen C, Le Borgne M. Toxicological risks of the cobalt–chromium alloys in dentistry: a systematic review. Materials. 2022;15(17):5801.
8. Ingole S, Pawar S, Gunukula S, Melath AJ, Pasha Z, Dumont NV, Bidkar K. Peri-implant soft tissue response to different abutment materials: A

randomised controlled clinical trial. Bioinformation. 2026;22(2):1170.

9. Kajiwara N, Masaki C, Mukaibo T, Kondo Y, Nakamoto T, Hosokawa R. Soft tissue biological response to zirconia and metal implant abutments compared with natural tooth: microcirculation monitoring as a novel bioindicator. Implant Dent. 2015;24:37-41.
10. Kanneganti KC, Vinnakota DN, Pottem SR, Pulagam M. Comparative effect of implant-abutment connections, abutment angulations, and screw lengths on preloaded abutment screw using three-dimensional finite element analysis: an in vitro study. J Indian Prosthodont Soc. 2018;18:161-7.
11. Kohal RJ, von Schierholz C, Nold J, Spies BC, Adolfsson E, Vach K, et al. Influence of loading and aging on the fracture strength of an injection-molded two-piece zirconia implant restored with a zirconia abutment. Clin Oral Implants Res. 2023;34:105-15.
12. Lee JH, Jang HY, Lee SY. Finite element analysis of dental implants with zirconia crown restorations: conventional cement-retained vs. cementless screw-retained. Materials. 2021;14:2666.
13. Naveau A, Rignon-Bret C, Wulfman C. Zirconia abutments in the anterior region: a systematic review of mechanical and esthetic outcomes. J Prosthet Dent. 2019;121:775-81.
14. Önöral Ö. Marginal discrepancy of 3-unit Co-Cr metal copings fabricated with additive and subtractive manners: a comparative study. Niger J Clin Pract. 2020;23:1274-80.
15. Rimondini L, Cerroni L, Carrassi A, Torricelli P. Bacterial colonization of zirconia ceramic surfaces: an in vitro and in vivo study. Int J Oral Maxillofac Implant. 2002;17:793-798.
16. Salihoglu U, Boynuegri D, Engin D, Duman AN, Gokalp P, Balos K. Bacterial adhesion and colonization differences between zirconium oxide and titanium alloys: an in vivo human study. Int J Oral Maxillofac Implant. 2011;26:101-107.
17. Scarano A, Piattelli M, Caputi S, Favero GA, Piattelli A. Bacterial adhesion on commercially pure titanium and zirconium oxide disks: an in vivo human study. J Periodontol. 2004;75:292-296.
18. Schulz KF, Altman DG, Moher D, CONSORT Group. CONSORT 2010 Statement: updated guidelines for reporting parallel group randomized trials. Trials. 2010;11:32.
19. Şen N, Şermet I, Gürler N. Sealing capability and marginal fit of titanium versus zirconia abutments with different connection designs. J Adv Prosthodont. 2019;11(2):105.
20. Van Eekeren P, Tahmaseb A, Wismeijer D. Crestal bone changes in macrogeometrically similar implants with the implant-abutment connection at the crestal bone level or 2.5 mm above: a prospective randomized clinical trial. Clin Oral Implant Res. 2015;27(12):1479-1484.
21. Zembic A, Sailer I, Jung RE, Siegenthaler D, Holderegger C, Hämmerle CH. Randomized controlled clinical trial of customized zirconia and titanium implant abutments for canine and posterior single-tooth implant reconstructions: preliminary results at 1 year of function. Clin Oral Implant Res. 2009;20:219-225.